HHS Public Access

Author manuscript

Pain. Author manuscript; available in PMC 2026 February 01.

Published in final edited form as:

Pain. 2025 February 01; 166(2): 448–459. doi:10.1097/j.pain.0000000000003394.

Persistent (NaV1.9) sodium currents in human dorsal root ganglion neurons

Xiulin Zhang[1,2], **Jane E Hartung**[1], **Michael S Gold**[1,*]

[1]Department of Neurobiology, and the Pittsburgh Center for Pain Research University of Pittsburgh School of Medicine, Pittsburgh, PA, United States

[2]Department of Urology, the Second Hospital of Shandong University, 250032, P.R. China

Abstract

NaV1.9 is of interest to the pain community for a number of reasons, including the human mutations in the gene encoding NaV1.9, *SCN11a*, that are associated with both pain and loss of pain phenotypes. However, because much of what we know about the biophysical properties of NaV1.9 has been learned through the study of rodent sensory neurons, and there is only 76% identity between human and rodent homologs of *SCN11a*, there is reason to suggest that there may be differences in the biophysical properties of the channels in human and rodent sensory neurons, and consequently, the contribution of these channels to the control of sensory neuron excitability, if not pain. Thus, the purpose of this study was to characterize NaV1.9 currents in human sensory neurons and compare the properties of these currents to those in rat sensory neurons recorded under identical conditions. Whole cell patch techniques were used to record NaV1.9 currents in isolated sensory neurons in vitro. Our results indicate that several of the core biophysical properties of the currents including persistence and a low threshold for activation are the conserved across species. However, we noted a number of potentially important differences between the currents in human and rat sensory neurons including a lower threshold for activation, higher threshold for inactivation, slower deactivation, and faster recovery from slow inactivation. Human NaV1.9 was inhibited by inflammatory mediators, while rat NaV1.9 was potentiated. Our results may have implications for the role of NaV1.9 in sensory, if not nociceptive signaling.

Introduction

Voltage-gated sodium channels (VGSCs) are generally thought of in the context of action potential generation and propagation, and eight of the nine VGSC alpha subunits expressed in mammalian tissues have been shown to contribute to action potential generation and/or propagation [6]. However, the ninth VGSC alpha subunit, NaV1.9, appears to be so slowly activating and inactivating [7; 22], at least at room temperature [40], that it appears to play

*Corresponding author: Michael S Gold, University of Pittsburgh, 203 Lothrop St, BST W1451, Pittsburgh, PA 15213, msg22@pitt.edu.

Author contributions: XZ, JEH and MSG contributed to the experimental design, collected and analyzed data. XZ wrote the first draft of the manuscript. XZ, JEH, and MSG contributed to all subsequent revisions of the manuscript.

Competing interests: None

None of the authors have a financial conflict of interest with any of the data in this manuscript.

a very different role in the control of neuronal excitability, largely impacting the resting membrane potential, and therefore only indirectly influencing action potential generation [9]. Nevertheless, NaV1.9 has remained a channel of interest to the pain research community for a number of reasons. First, it is only expressed in the peripheral sensory [10] and enteric [33; 37] neurons, and appears to be enriched in putative nociceptive afferents responsible for pain associated with tissue injury [12]. Second, NaV1.9 currents are increased by proinflammatory mediators [2; 3; 16; 27; 38], suggesting that NaV1.9 contributes to the sensitization of nociceptive afferents thought to underlie inflammatory hyperalgesia. Third, while data from NaV1.9 null mutant mice suggests the channel contributes little to baseline nociceptive thresholds [35], consistent with the data from isolated neurons and ex-vivo preparations [16], it appears to contribute to hypersensitivity evoked by pro-inflammatory mediators [16; 38], as well as complete Freund's adjuvant-induced inflammation [35], or supernatant from inflamed human tissue applied to the gut [16]. In the skin, NaV1.9 appears to play a more prominent role in heat than mechanical hypersensitivity [34; 35], while in the gut, NaV1.9 contributes to hypersensitivity to slow rather than rapid stretch of the colon [16]. Finally, mutations in *SCN11a*, the gene encoding NaV1.9, are associated with both loss of function (insensitivity to pain) and gain of function (chronic pain) phenotypes [9]. The contribution of NaV1.9 to neuropathic pain has yet to be fully characterized with largely negative results in preclinical studies ([34; 35], but see [24; 26]), and a gain of function mutation of NaV1.9 associated with neuropathic pain patients [19]. Taken together, these data suggest NaV1.9 may play a particularly important role in inflammatory hypersensitivity in both animal models and humans.

Despite its potential importance in inflammatory if not neuropathic pain syndromes, virtually all that is known about the biophysical and pharmacological properties of NaV1.9 currents has been obtained through the study of rodent sensory neurons and heterologous expression systems. There is a report of NaV1.9 currents in human DRG neurons, in which recordings were obtained from 14 neurons, nine of which had measurable levels of persistent (NaV1.9-like) currents [11]. Yet given that rat and mouse homologs of *SCN11a* share only 76% identity with human *SCN11a* [8; 22], species differences in both biophysical and pharmacological properties should not be surprising [22]. Furthermore, given evidence of the impact of heterologous expression systems on the biophysical and pharmacological properties of VGSCs [29], it is important to characterize VGSCs in their native environment. Thus, the goal of the present study was to characterize NaV1.9 currents in human DRG neurons.

Materials and Methods:

Human Subjects

Data were obtained from the L4 and L5 DRG recovered from 33 human organ donors with the consent of family members for the use of their loved one's tissue for research purposes. All procedures were approved by the University of Pittsburgh Committee for Oversight of Research and Clinical Training Involving Decedents.

Collection of human DRGs

The detailed methods for collection of L4 and L5 DRGs have been described in our previous reports ([15; 30; 31; 41–43]). Briefly, after L4 and L5 ganglia were recovered, the ganglia were placed in ice cold collection media with the following composition: 129.5 mM NaCl, 5 mM KCl, 1.2 mM MgCl2, 30 mM HEPES, 2.5 mM glucose and 0.23% phosphoric acid adjusted with Tris Base to a pH of 7.35.

Isolation of human DRG neurons

The protocol employed has been described in our previous studies ([31]). Briefly, ganglia were cut into small (~2–5 mm^3) pieces and transferred to collection media containing 1 mg/mL of collagenase P (Roche Bioscience), 1 mg/mL of Trypsin (TRL, Worthington) and 0.1 mg/mL DNase 1 (Roche Bioscience), and placed on a shaking tray in a 37°C water bath. Fresh enzyme solution was added every 90 minutes. The enzymatic treatment was terminated when pieces of ganglia began to visibly fall apart. Pieces of ganglia were transferred to a 15 mL tube and mechanically dissociated through a fire-polished Pasteur pipette. Enzymatic activity was quenched by adding 7 mL of collection media supplemented with 2 mg/mL soybean trypsin inhibitor (type II, Sigma-Aldrich), 1 mg/mL bovine serum albumin (Sigma-Aldrich), fetal bovine serum (to a final concentration of 10%, Hyclone), and 2 mM $CaCl_2$, and dispersed cells were centrifuged at 450G for 4 minutes. The pellet was re-suspended in a Leibovitz L-15 (Invitrogen) based media (basal media) containing (per 500 mL): 60 mg imidizole, 15 mg aspartic acid, 15 mg glutamic acid, 15 mg cystine, 5 mg β-alanine, 10 mg myo-inositol, 10 mg choline-Cl, 5 mg p-aminobenzoic acid, 25 mg fumaric acid, 2 mg vitamin B12 and 5 mg of lipoic acid. All chemicals used to supplement the L-15 media were obtained from Sigma-Aldrich. Cells were spun again for 4 minutes at 450G, the pellet was then resuspended in 1 mL of basal media. This was loaded on a Percoll (Sigma-Aldrich) gradient, and spun at 1800G for 10 min. The pellet was resuspended in complete media which was composed of basal media diluted 1:10 with fetal bovine serum and then supplemented to yield a final concentration of 50 ng/mL nerve growth factor (NGF 2.5S, Invitrogen), 0.3 mg/mL glutamine (Invitrogen), 0.225 mg/mL glucose (Sigma-Aldrich), 2.55 mg/mL ascorbic acid (Sigma-Aldrich), and 0.12 mg/mL glutathione (Invitrogen), and 0.2% (w/v) $NaHCO_3$ (Sigma-Aldrich). Cells were plated onto poly-L-lysine coated glass coverslips (Invitrogen) placed in CO2 (5%) incubator at 37℃ for 4h prior to flooding with Complete Media. Neurons were studied between 4 and 72 h in culture.

Isolation of rat TG and DRG neurons

Adult (250–320 g) male and female Sprague-Dawley rats (Envigo, Indianapolis, IN)) were used for all experiments. Adult rat DRG and trigeminal ganglia (TG) were surgically obtained, enzymatically treated and mechanically dissociated as previously described [25]. Cells were also plated on poly-L-lysine coated glass coverslips (Invitrogen), which were placed in 35 mm culture dishes and stored in a CO_2 (5%) incubator at 37˚C for 2 hr prior to flooding with Complete Media. Neurons were studied between 4 and 48h of plating.

Patch clamp recording

Whole-cell patch-clamp recordings were performed with an Axopatch 200B controlled with pClamp (v10.2) software (Molecular Devices, Carlsbad, CA) in combination with a Digidata 1320A A/D converter (Molecular Devices) or with a HEKA EPC10 controlled with Patchmaster software (v2×90.2). Data were acquired at 10–20 kHz and filtered at 2 kHz. Borosilicate glass (WPI, Sarasota, FL) electrodes were 1–1.5 MΩ were filled with an electrode solutions containing (in mM): CsF 100, TEA-Cl 40, NaCl 5, CaCl 2 1, EGTA 11, HEPES 10, Mg-ATP 2, and GTP 1; pH was adjusted to 7.2 with Tris-base and osmolality was adjusted to 310 mOsm with sucrose. The bath solution consisted of (in mM): NaCl 35, CholineCl 65, TEA-Cl 30, CaCl2 0.1, MgCl2 5, CdCl2 0.1, HEPES 10, and glucose 10; pH was adjusted to 7.4 with Tris-Base, and the osmolality adjusted to 320 with sucrose. Capacitive currents were minimized with amplifier circuitry. Series resistance compensation was always employed, and if it was not possible to achieve compensation greater than 75%, neurons were not included for further analysis. Similarly, if estimated voltage errors were greater than 5 mV, data were not included for further analysis, where voltage errors were estimated based on the peak inward current across the uncompensated series resistance.

Steady-state properties: The voltage-dependence of current activation and inactivation was determined with standard current-voltage (I-V) and steady-state inactivation (H-infinity) protocols. Neurons were held at −120 mV, total TTX-R I-V curves were generated in the presence of 300 nM TTX unless indicated with a series of 50 ms test pulses between −110 and −10 mV, evoked every 5 seconds (Figure 1A), then I-V curves (NaV1.8 mediated) were evoked at a holding potential of −50 mV to inactivate NaV1.9. NaV1.9 currents were isolated from NaV1.8 currents post-hoc, via digital subtraction of the NaV1.8 I-V curves from the total to obtain NaV1.9 I-V curves. In a subpopulation of neurons, the putative NaV1.8 selective blocker A-803467 was used to block NaV1.8 currents. Of note, it was necessary to use 10 μM A-803467 to block NaV1.8 currents in human DRG neurons. Steady-state inactivation/availability curves were obtained with a voltage protocol in which currents were evoked by a voltage step to −50 mV following a series of 500 ms pre-pulses from −120 to −10 mV, the pre-pulse was increased by 10 mV increments every 5 seconds.

Kinetics: The time constant (tau) of current activation was determined with a single exponential fitted to the rise phase of the current following depolarizing voltage-steps, where the voltage-dependence of current activation was determined from the currents evoked with the I-V protocols. The time constant (tau) of current inactivation was determined with a single exponential fitted to the decay phase of the evoked current during sustained (500 ms) voltage steps, where the current evoked during the conditioning voltage step used for the generation of steady-state inactivation curves was most often used for this purpose. The time constant (tau) of current deactivation was determined with a single exponential fitted to the decay phase of the evoked current following a repolarizing voltage-step following current activation with a voltage step to −50 mV. To determine the recovery of NaV1.9 currents from slow inactivation, currents were evoked at −50 mV from a holding potential of −120 mV at 0.3 Hz following three minutes at a holding potential of −50 mV.

Temperature dependence: Given a previous report suggesting that NaV1.9 currents may be particularly sensitive to increases in temperature, currents in neurons from a subgroup of donors were studied at room temperature (~20°C) and at 34°C (and in a smaller group of neurons at 37°C). Temperature was controlled with a feedback-controlled resistive heater in line with the perfusion system, where the thermocouple was positioned ~200 μm from the neuron studied. For comparative purposes, we assessed the impact of temperature controlled in the same manner on the properties of TTX-S and NaV1.8 currents.

Impact of local anesthetics: Given the importance of local anesthetics to pain control we sought to assess the impact of the canonical local anesthetic lidocaine on persistent currents in human DRG neurons. A 150 ms test pulse to −50mV from a holding potential of −120 mV was applied in each neuron to evoke NaV1.9 current, and lidocaine at concentrations of 0.1 to 3mM was applied.

Inflammatory mediators: Finally given evidence of a role for NaV1.9 in inflammatory hyperalgesia, we sought to assess the impact of an inflammatory soup consisting of PGE2, bradykinin, serotonin, and histamine on persistent currents. The inflammatory soup was applied after establishment of a stable baseline.

Test agents: All salts used for electrophysiological recording were obtained from Sigma-Aldrich. TTX (Sigma-Aldrich) was dissolved in distilled water (dH2O) as a 1 mM stock solution, and stored at 4°C until use. Prostaglandin E2 (Sigma-Aldrich) was dissolved in ethanol as a 10 mM stock solution and stored at −20°C until use. Bradykinin was dissolved in 1% acetic acid in a10 mM stock concentration and stored at −20°C until use. Lidocaine was prepared as a 10 mM stock solution with 5 mM Na-HEPES buffered dH2O, with a pH adjusted to 7.0 with TEA-OH, and stored at −20°C until use. Drugs were diluted to final concentrations in bath solution from stock solutions at least 1000 times greater than the highest concentration employed.

Data analysis: Amplifier circuitry was used to estimate membrane capacitance. Tail currents evoked following membrane repolarization to −120 mV in association with the I-V protocol, were used to generate conductance-voltage plots. Steady-state inactivation and G-V curves were fitted with modified Boltzmann equations so as to determine maximal conductance (G_{max}), the voltage at which currents were either half inactivated or half activated ($V_{0.5}$), as well as the slopes of the two curves. Lidocaine concentration-response curves were fitted with a modified Hill equation to enable estimation of the concentration needed to block 50% of evoked current.

All pooled data are presented as mean ± standard error of the mean. Unless otherwise stated, a t-test was used for statistical comparisons between human and rat data, where a difference with $p < 0.05$ was considered statistically significant.

Results

Neurons included in this study were obtained from 33 donors (21 males and 12 females). The average age of the males was 38.8 years (range = 17–64 years) while that of females

was 41.8 years (range = 17–61 years). The average membrane capacitance of the 144 human DRG neurons included in this study (i.e., those in which >200 pA of low threshold persistent current was detected) was 149.5 ± 5.0 pF, with a range from 42.97 to 366.2 pF. The average neuron capacitance per donor was 153.0 ± 4.8 pF. While rat neurons were not systematically analyzed for the presence of low threshold persistent current across all cell body sizes, average capacitance of rat neurons in which persistent current was detected was 32.0 ± 1.3 pF (n = 138, $p < 0.01$). The average neuron capacitance per rat was 32.3 ± 1.9 pF (n = 25, $p < 0.01$). Consistent with previous reports, rat DRG neurons with NaV1.9 current tended to be small with a cell body diameter < 27 μm. In contrast, NaV1.9 currents were found in human DRG neurons of all sizes with a range that spanned the smallest to the largest neurons studied. Nevertheless, of the 21 human DRG neurons with persistent current tested for capsaicin (300 nM) sensitivity, 16 were capsaicin responsive, suggesting most of the human neurons with persistent current are putative nociceptors. Of note, while we have previously described a time in culture dependent increase in TTX-S and the more rapidly inactivating TTX-R currents in human sensory neurons [42], there was not significant influence of time in culture on NaV1.9 current density which was −47.3 ± 5.1 pA/pF on day 0, −64.2 ± 5.7 pA/pF on day 1, but only −52.8 ± 7.2 pA/pF on day 2.

Biophysical properties of NaV1.9 currents in human and rat sensory neurons

Recordings were made in solutions chosen to minimize potential contamination of voltage-gated Na+ currents by voltage-gated K+ or Ca2+ currents. To facilitate clamp control of voltage-gated Na+ currents, extracellular Na+ was reduced to 35 mM. TTX-sensitive Na+ currents are completely blocked in the presence of 300 nM TTX, which allowed us to record TTX-R Na+ current in isolation. Two approaches were used to isolate NaV1.9 from NaV1.8 currents. One was voltage, where a depolarized holding potential (to ~−50 mV) enabled complete inactivation of NaV1.9 channels, but the full availability of NaV1.8 channels. Any inactivation of NaV1.8 currents at −50 mV could be rapidly recovered with a brief (10 ms) hyperpolarizing voltage step to −60 or −70 mV. This allowed digital subtraction of NaV1.8 currents from the total current evoked from a holding potential of −120 mV, leaving NaV1.9 currents in isolation (Figure 1A). The second approach was with A-803467, which at 10 μM (but not 300 nM), completely blocked NaV1.8 in human DRG neurons (Figure 1B). The currents isolated by both methods evoked from human and rat sensory neurons were grossly comparable, and had a low threshold for activation, demonstrated little fast inactivation at voltage steps >−50 mV, and were comparatively slowly inactivating at voltage steps to more depolarized potentials.

I-V data were collected from 120 human DRG neurons and 89 rat DRG and TG neurons under the same conditions with the same series of protocols. Pooled I-V data normalized to cell capacitance (Figure 1C) revealed a species difference in current density, which was much greater in rat sensory neurons despite the relatively large variability in current density from neuron to neuron. This variance is illustrated in a plot of the current density at −50 mV, where the violin plot is used to illustrate the distribution of current density at −50 mV per cell (with an n = 144 for human and 138 for rat, respectively. This “n” is larger than that for which there were complete I-V data, as some neurons were only studied with a test-pulse to

−50 mV) and the dot-plot overlaying the violin plot are of the mean current density per rat (n = 25) or human donor (n = 33) (Figure 1C inset).

While difficult to see in the I-V plots, G-V plots normalized to maximal conductance revealed a species difference in the voltage-dependence of current activation as well, which was more hyperpolarized in human DRG neurons. G-V data for each neuron was fitted with a Boltzmann equation to determine G_{max}, and this fitted value was subsequently used to normalize each G-V curve prior to pooling. As with Figure 1C, variability in the G-V plots is illustrated in the inset to Figure 1D, where the violin plots include data from single neurons and the overlaying dot plots are average values from individual humans or rats. The $V_{0.5}$ for activation in human DRG neurons was −63 ± 1.3 mV (n = 30 donors), while that in rat sensory neurons was −58 ± 0.9 mV (n = 25 rats). The difference in $V_{0.5}$ of activation between groups is significant ($p < 0.05$). However, there were no differences between groups with respect to the slope of the G-V curves, which was 6.7 ± 0.3 (n = 32) and 6.9 ± 0.3 (n = 25) mV/e-fold change in conductance in sensory neurons from human and rat, respectively.

While no power analyses were performed prior to the start of this study to determine the number of donors needed to detect an influence of demographic or other donor variables on current density, we did perform a post-hoc analyses to assess the potential influence of sex, age, and whether the donor had evidence of an opioid use disorder. Given that the rats used in the study were largely a convenience sample where neurons were recovered from otherwise healthy adult rats to be used for other purposes, comparable analyses were not performed on rat neurons. We detected no influence of sex on current density which had a median of −51.5 pA/pF in females (n = 7) and −54.0 pA/pF in males (n = 21, $p > 0.05$ Mann-Whitney Rank Sum Test). Nor was there evidence of an influence of age on current density when donors were analyzed by those younger than 30 and older than 60, where the median was −47.0 in the young (n = 7) and −35.3 in the old (n = 4). Finally, there was no evidence of an influence of an opioid use disorder (OUD) as the density of NaV1.9 current in those without evidence of an OUD was −47.6 pF/pF (n = 20), while that in donors with evidence of an OUD was −56.5 pF/pA (n = 20). We were able to assess the influence of ganglia (TG vs DRG) in rat, and no significant influence of ganglia was detected: The median current density was −107 pA/pF in TG (n = 6) and −120.4 pA/pF in DRG (n = 19).

The voltage-dependence steady-state inactivation was qualitatively similar in human (n = 70 neurons from 15 donors) and rat (n = 78 neurons from 13 rats) sensory neurons (Figure 2A). However, there was a significant difference between human and rat neurons in the $V_{0.5}$ for inactivation (−44.8±1.1 mV in human vs −53±1.9mV in rat; $p < 0.01$) (Figure 2B). The variability in the $V_{0.5}$ for inactivation is illustrated in the inset to Figure 2B, with data plotted as in Figure 1. There was a significant species difference with respect to the fraction of current resistant to steady-state inactivation, which was larger in human neurons (15 ± 2.7% vs 9 ± 2.2%, $p<0.05$). There was also a small but significant species difference in the slope of steady-state inactivation curves which was 9.6 ± 0.6 and 8.1 ± 0.3 mV/e-fold decrease in current availability in human and rat sensory neurons, respectively ($p = 0.04$).

The kinetics of NaV1.9 current were evaluated with the time constants obtained by a single exponential equation fitted to the rising (activation), decay during sustained depolarization

(inactivation), and tail currents evoked during with voltage-steps to potentials at which channels were closed (deactivation) of NaV1.9 currents (Figure 3). Current evoked with the protocol used for the generation of I-V/G-V curves were used to determine the voltage-dependence of the kinetics of current activation. The current evoked during the conditioning voltage-step in the steady-state inactivation protocol and or during the I-V curve was used to determine the voltage-dependence of the kinetics of current inactivation. A tail current protocol involving a voltage-step to −50mV to evoke NaV1.9 currents, followed by a voltage step to test potentials ranging from −120 to −80mV, was used to determine the voltage-dependence of the kinetics of deactivation.

There was no statistically significant species difference in the kinetics of current activation, when data were analyzed per donor or rat (Figure 3A and B) which had a time constant of 6.8 ± 0.4 and 7.9 ± 0.6 at −50 mV in sensory neurons from human and rat, respectively. The variance in the kinetics of activation is illustrated in the inset to Figure 3B with data plotted as per the insets to Figure 1.

There was a small but significant species difference in the kinetics of inactivation which was faster at just about every voltage step in the rat, despite the hyperpolarizing shift in the voltage-dependence of current activation in human DRG neurons (Figure 3C). The variability in this endpoint is illustrated in the data obtained with voltage-steps to −40 mV because it was not possible to detect any inactivation in so many human DRG neurons at −50 mV over the 500 ms voltage step used in the inactivation protocol. Data in the inset to Figure 3C are plotted as in previous figures.

There was also a significant species difference in the kinetics of current deactivation which again was faster in sensory neurons from rat than human (Figure 3D). While data for the full tail-current protocol was only collected on neurons from three humans and three rats, tail currents associated with a voltage step to −120 mV following a test pulse to −50 mV was collected in the majority of neurons studied where the average rate of deactivation was 1.55 ± 0.07 ms/neurons (n = 114) and 1.56 ±0.12 per donor (n = 27) for human sensory neurons and 1.0 ± 0.04 ms/neuron (n = 129) and 1.01 ± 0.07 ms per rat (n = 25) for rat sensory neurons (Figure 3D inset). Researchers have reported slow recovery from inactivation for NaV1.9 in human and rodent DRG neurons [7; 11]. To examine recovery of NaV1.9 current from slow inactivation, NaV1.9 currents in human and rat sensory neurons were evoked at −50 mV from a holding potential of −120 mV at 0.2 Hz, following three minutes at a holding potential of −50 mV (Figure 4A). NaV1.9 currents in human DRG neurons recovered fully from slow inactivation over a process best fitted with a sigmoidal equation, with an average slope of recovery of 95.2 ± 12 s (n = 36 neurons) and a median recovery to 90% of max of 127 s (87 and 182 are the 25th and 75th percentiles). Interestingly, there appeared to be three subpopulations of neurons that could be defined by the time course of recovery (Figure 4B), with the majority 25 of 36, exhibiting a fast recovery from inactivation (recovery to 90% of max in 100 ± 5.8 s), with smaller subpopulations requiring with medium (200 ± 18 s to 90%, n = 6) and slow (349 ± 3.5 s to 90%, n = 5) rates of recovery. In contrast, NaV1.9 currents in rat sensory neurons recovered over a process best fitted with a single exponential (Figure 4C). While not as clearly defined as the three subpopulations of neurons in human, there appeared to be three subpopulations

of rat sensory neurons as well that could be differentiated based on the time-course of the recovery from slow inactivation. In contrast to human DRG neurons, the recovery from slow inactivation in rat sensory neurons was best fitted with a single exponential equation (rising to max), with an average time constant of 245.8 ± 46 s, and a median time to 90% of max of 178s (117 and 257); this median time to 90% of max was significantly slower than that in human DRG neurons ($p = 0.01$, Mann Whitney Rank Sum Test). Consistent with this difference, NaV1.9 currents in the majority of sensory neurons from the rat (16 of 30) recovered slowly (287 ± 24 s to 90% of max), while others had a medium (127 ± 7.8 s to 90%, $n = 8$) and fast (60.5 ± 4.2 s, $n = 6$) rate of recovery. The differences in the proportion of neurons with fast, medium, and slow rates of recovery in human and rat sensory neurons was significant ($p < 0.01$, Chi-Square).

The influence of elevated temperature on NaV1.9 currents

While NaV1.9 was originally considered to function as a subthreshold current [7], more recent evidence from mice suggests that at more physiological temperatures, the kinetics of current activation and inactivation are increased to the point that NaV1.9 contributes to action potential generation [40]. There is also a dramatic increase in current density at more physiological temperatures. To determine the extent to which NaV1.9 currents in human DRG neurons are comparably temperature sensitive, we assessed the impact of raising the bath temperature to 34°C. In some neurons, the temperature was subsequently raised to 37°C, to rule out the possibility that the relatively small changes observed in kinetics and density were due to a particularly steep and narrow temperature dependence. Currents were studied in 21 neurons from 5 donors. Increasing the bath temperature from 20°C to 34°C was associated with a small but significant increase in the density of current evoked at −50 mV (Figure 5A), from −40.7 ± 5.8 pA/pF to −56.5 ± 9.5 pA/pF, for a 42.1 ± 7.5% increase (Figure 5A). Importantly, the increase an increase in current density was detected in every neuron tested. The increase in current density was not due to a hyperpolarizing shift in the voltage-dependence of current activation, as is seen by the largely overlapping G-V curves generated from current evoked at 20°C and 34°C (Figure 5B). However, the increase in current density was associated with an increase in the current activation and deactivation rates (Figure 5C). The activation rate increased from 6.3 ± 0.5 ms to 3.0 ± 0.3 ms at −50 mV, for more than a 50% decrease (51.7 ± 3.7%) in the tau of current activation ($p < 0.01$). The rate of current deactivation dropped from 1.03 ± 0.06 ms to 0.54 ± 0.05 ms, for a 47 ± 3.7% decrease in the tau of current deactivation ($p < 0.01$). However, the small hyperpolarizing shift in current inactivation (Figure 5D), was not significant. Comparable changes were observed in NaV1.9 currents from rat DRG neurons (Figure 5A inset).

In the face of relatively small changes in NaV1.9 currents when the bath temperature was increased from 20°C to 34°C, we sought to determine whether TTX-S I_{Na} and TTX-R I_{Na} (i.e., NaV1.8) may be comparably resistant to temperature. TTX-S and TTX-R I_{Na} were isolated by changing a 500 ms prepulse potential to −100 mV from a holding potential of −50 mV (to inactivate NaV1.9, Figure 6A), and currents were evoked in the same neurons at 20oC and 34oC (Figure 6A). There were significant increases in peak TTX-R and TTX-S I_{Na} density from −33.0 ± 4.3 to −47.4 ± 5.9 ($p < 0.01$) and from −44 ± 5.3 pA/pF to −68.4 ± 7.4 pF/pF ($p < 0.01$), respectively (Figure 6B). The increase in current

density was associated with an increase in the rate of current activation (Figure 6C) and inactivation (Figure 6D) as reflected by a decrease in the time constants (Tau) of activation and inactivation for both TTX-R and TTX-S I_{Na} (although there was a subpopulation of neurons in which the activation rate appeared to slow). While not assessed in TTX-S INa, the rate of deactivation was also increased for TTX-R I_{Na} (Figure 6E).

The impact of lidocaine on NaV1.9 currents in human DRG neurons

Given the importance of local anesthetics for local and regional anesthesia we next sought to assess the impact of the prototypical local anesthetic, lidocaine, on NaV1.9 currents in human DRG neurons. Seven neurons from three donors were challenged with concentrations of lidocaine ranging from 0.1 to 3 mM. Peak evoked current at −50 mV in the presence of lidocaine was analyzed as a fractional block, relative to the peak current evoked prior to the application of lidocaine (Figure 7A). Pooled data were fitted with a modified Hill equation to yield an IC_{50} of 0.93 mM (Figure 7B). This value is considerably higher than our previous estimates for the lidocaine induced block of TTX-S and TTX-R I_{Na} in rat DRG neurons, which were 50.2 ± 8.2 μM and 119.5 ± 25 μM, respectively [13].

Modulation of NaV1.9 currents by inflammation mediator in rat and human DRG neurons

Inflammatory mediators such as bradykinin, ATP, histamine, prostaglandin E2, and norepinephrine have been reported to potentiate NaV1.9 current in rodent DRG neurons and contribute to the hyper-excitability of nociceptors observed during inflammatory pain [1; 16; 27; 38]. To examine whether inflammatory mediators can potentiate NaV1.9 current in human DRG neurons, an inflammatory soup (IS) consisting of PGE2 (1 μM), histamine (1 μM), bradykinin (10 μM), and serotonin (1 μM) or control vehicle (0.1% ethanol) was applied to neurons while NaV1.9 current was evoked at −50 mV every 5 seconds. While vehicle had no effect on NaV1.9 current (n=7), IS produced a 50% decrease in current amplitude in 7 of 8 neurons tested (Figure 8A). Pooled G-V data from these neurons suggested that the decrease was due to a drop in peak conductance rather than a depolarizing shift in channel activation (Figure 8B). In contrast to the largely inhibitory influence of IS on NaV1.9 in human DRG neurons, IS resulted in an increase in NaV1.9 currents in 4 of 4 rat DRG neurons tested from two preparations. Vehicle had no detectable influence on NaV1.9 currents in 6 of 6 rat DRG neurons tested (Figure 8C).

Discussion:

In the present study we compared the biophysical and pharmacological properties of NaV1.9 in human and rat sensory neurons. Our results indicate that while the current properties are qualitatively similar in the two species, there are potentially important differences. These include the distribution of the channel among sensory neurons, current density, voltage-dependence of current activation, voltage-dependence of current inactivation, rates of current inactivation and deactivation, recovery from slow inactivation, and the impact of inflammatory mediators. In addition, we observed a relatively small impact of temperature on both human and rat NaV1.9 currents, largely associated with faster kinetics of activation and inactivation which were comparable in magnitude to the changes observed in human TTX-S and TTX-R I_{Na} currents. Finally, we observed a relatively low potency lidocaine-

induced block of NaV1.9 currents. Our results suggest that while still potentially important in pain, NaV1.9 channels in human DRG neurons may play a larger role in the control of sensory neuron excitability.

Distribution of NaV1.9

Initial reports of NaV1.9 suggested it was preferentially expressed in putative nociceptive sensory neurons based on its expression in small-diameter rat [10; 39] and mouse [32] TG and DRG neurons. RNAseq analysis confirmed that NaV1.9 is enriched in subpopulations of putative nociceptive human DRG neurons, but more widely expressed in multiple subpopulations of sensory neurons [5]. Initial electrophysiological analysis of human DRG neurons confirmed the presence of NaV1.9 currents in small diameter (<30 μm) neurons, although only small diameter neurons were studied [11]. Extending these initial observations we confirmed NaV1.9 currents are present in many (16 of 21) putative nociceptive afferents as defined by capsaicin (300 nM) sensitivity. However, in contrast to the distribution of mRNA encoding NaV1.9, there was little evidence that functional protein was enriched in small diameter human DRG neurons. There was a trend toward a significant negative correlation between cell body capacitance and current density ($p = 0.051$), but with an R^2 of 0.03. The fact that NaV1.9 currents were detected in >80% of neurons tested from each donor, regardless of cell body diameter suggests that NaV1.9 may play a larger role in the control of sensory neuron excitability. Interestingly, the density of NaV1.9 currents was relatively stable across donors analyzed by sex, age, or evidence of an opioid-use disorder, suggesting that changes in nociceptive processing observed in these different groups of people are not due to regulation of NaV1.9 current density.

Biophysical properties of human NaV1.9

The dramatically higher current density in rat sensory neurons would suggest the channel plays a more prominent role in the control of sensory neuron excitability in the rat. However, the more hyperpolarized G-V curve in human DRG neurons, combined with the more depolarized inactivation curve indicates that this current contributes to the establishment of resting membrane potential over a broader voltage range in human sensory neurons. Furthermore, the slower rates of current inactivation and deactivation suggest that the current contributes a depolarizing drive over longer periods, and that following an action potential, the current would play a larger role in driving the depolarization needed for a subsequent action potential. The faster rate of recovery from slow inactivation observed in most human DRG neurons would also facilitate the contribution of NaV1.9 to the excitability of human DRG neurons. Importantly, these differences would be maximized in axons and terminals, where differences in membrane capacitance between rat and human sensory neurons are not as large as at the cell soma. Thus, despite the smaller current density in human DRG neurons, the biophysical properties of the current in human DRG neurons suggest the channel may play a larger role in controlling neuronal excitability in the human than in the rat. Consistent with this suggestion, gain [4; 14; 18] and loss [20; 21] of function mutations in human NaV1.9 appear to have a far more pronounced pain phenotype than is observed in the complete knockout of NaV1.9 expression in mice [17; 23; 24; 28; 36].

While the only previous biophysical characterization of NaV1.9 currents in human DRG neurons involved a relatively limited data set, these authors did observe the hyperpolarized shift in the NaV1.9 G-V curve, relative to that in mouse DRG neurons [11]. The authors suggested that this difference in the G-V was due to differences in the amino acid sequences of the S4 segment [11], which could be responsible for differences in several of the other biophysical properties noted here.

Influence of Temperature

The observation that NaV1.9 may be particularly temperature sensitive [40] was intriguing for a number of reasons, including the implication that the contribution of NaV1.9 to sensory neuron excitability may change dramatically from the relatively cold distal appendages to parts of the neuron sitting at ~37°C. The greater than four-fold increase in current combined with the increase in the kinetics of channel activation at 37°C relative to 20°C suggested NaV1.9 may contribute to action potential generation [40]. Our failure to replicate these previous observations was not due to differences in the temperature range studied (i.e., 34°C vs 37°C, as suggested by Figure 5). Differences in results could be due to species differences, given that we used human and rat neurons, while mice were used previously. However, the fact that we also failed to replicate the largely negative impact of temperature on TTX-S and more strikingly TTX-R (NaV1.8) currents previously reported [40], argues against this possibility. That is, in contrast to the ~40% increase in TTX-R I_{Na} density we observed, Touska et al reported a 12% decrease in NaV1.8 when the bath temperature was increased from 20°C to 30°C. This would only leave the recording conditions as a possible explanation, where Touska et al used 140 mM Na+ in the bath solution used to record Na+ currents, while we reduced the extracellular Na+ concentration to 35 mM to maintain clamp control over the relatively large NaV currents in rat and human sensory neurons. Regardless, our results suggest that NaV1.9 in humans and rats contributes minimally to changes in nociceptor excitability in response to changes in ambient temperature, at least between 20°C and 37°C, and is unlikely to contribute directly to action potential generation at any temperature.

Impact of lidocaine

Because a relatively small number of neurons were studied with lidocaine with a relatively small number of concentrations, interpretation of our lidocaine results should be made with caution. Nevertheless, our results are largely consistent with those obtained from heterologously expressed human NaV1.9 channels, where the IC_{50} was 356 μM [22], considerably higher than that for block of NaV1.7 or NaV1.8 channels. Given efficacy of drugs like lidocaine for regional and local anesthesia, our results suggest it is unlikely that NaV1.9 channels contribute to directly action potential initiation or propagation.

Dynamic modulation of NaV1.9 by inflammatory mediators

The observation that NaV1.9 currents were decreased in seven of eight neurons tested, was a surprise given previous results in rodent sensory neurons [1; 3; 27]. These negative results should be viewed with caution, given both the small number of neurons tested and the possibility that the increase in current may develop more slowly [38]. We may have also failed use the right combination and/or concentration of mediators [27]. Nevertheless, our

results suggest that in contrast to rodents, NaV1.9 may not contribute to acute inflammatory hypersensitivity. On the other hand, given a primary role for NaV1.9 in the regulation of resting membrane potential, and consequently, an influence on excitability secondary to the influence on resting membrane, the impact of a change in NaV1.9 current density and/or voltage-dependence of activation, will depend on the biophysical properties of the other ion channels present in the cell membrane. Even a decrease in NaV1.9 current could lead to an increase in excitability under the right conditions. Consistent with this possibility is the observation that while a small depolarizing shift in the voltage-dependence of NaV1.9 activation is associated with an increase in pain [14], an larger shift in the voltage-dependence of NaV1.9 activation is associated with the loss of pain [20].

Conclusions

Consistent with a previous description of NaV1.9 currents in human DRG neurons [11] several of core biophysical features of these currents, including the low threshold for activation and its persistence are conserved across species. However, we noted a number of potentially important species differences were noted. Most striking among these was the response to inflammatory mediators, which largely decreased currents in human DRG neurons, but increased currents in rat neurons. Whether this difference in current regulation has a differential impact on neuronal excitability, will require further experimentation. However, given that the net effect a change in membrane potential will have on neuronal excitability, and consequently pain, will depend on the biophysical properties of all the other ion channels in the membrane, this observation raises the possibility that more species differences in the density and distribution of ion channels controlling sensory neuron excitability have yet to be revealed. Taken together, these results highlight yet again the importance of the use of human tissue for the validation of potential therapeutic targets prior to the initiation of costly phase I trials.

Acknowledgements:

The authors would like to thank Vidhya Nagarajan, Hannah Hathaway, Chris Scott for technical assistance, the team at the Center for Organ Recovery and Education for their outstanding work in facilitating the recovery of human tissue for research purposes, and most importantly the family of the loved ones whose tissue was used in this study. This work supported by NIH Grants 1R01DE018252 (MSG), R01 NS122784 (MSG), RM1 NS128775 (MSG), and F32NS103231 (JEH).

Data and materials availability:

Yes

References:

[1]. Amaya F, Wang H, Costigan M, Allchorne AJ, Hatcher JP, Egerton J, Stean T, Morisset V, Grose D, Gunthorpe MJ, Chessell IP, Tate S, Green PJ, Woolf CJ. The voltage-gated sodium channel Na(v)1.9 is an effector of peripheral inflammatory pain hypersensitivity. J Neurosci 2006;26(50):12852–12860. [PubMed: 17167076]

[2]. Baker MD. Protein kinase C mediates up-regulation of tetrodotoxin-resistant, persistent Na+ current in rat and mouse sensory neurones. J Physiol 2005;567(Pt 3):851–867. [PubMed: 16002450]

[3]. Baker MD, Chandra SY, Ding Y, Waxman SG, Wood JN. GTP-induced tetrodotoxin-resistant Na+ current regulates excitability in mouse and rat small diameter sensory neurones. J Physiol 2003;548(Pt 2):373–382. [PubMed: 12651922]

[4]. Baker MD, Nassar MA. Painful and painless mutations of SCN9A and SCN11A voltage-gated sodium channels. Pflugers Arch 2020;472(7):865–880. [PubMed: 32601768]

[5]. Bhuiyan SA, Xu M, Yang L, Semizoglou E, Bhatia P, Pantaleo KI, Tochitsky I, Jain A, Erdogan B, Blair S, Cat V, Mwirigi JM, Sankaranarayanan I, Tavares-Ferreira D, Green U, McIlvried LA, Copits BA, Bertels Z, Del Rosario JS, Widman AJ, Slivicki RA, Yi J, Woolf CJ, Lennerz JK, Whited JL, Price TJ, Gereau RWt, Renthal W. Harmonized cross-species cell atlases of trigeminal and dorsal root ganglia. bioRxiv 2023.

[6]. Catterall WA, Goldin AL, Waxman SG. International Union of Pharmacology. XLVII. Nomenclature and structure-function relationships of voltage-gated sodium channels. Pharmacol Rev 2005;57(4):397–409. [PubMed: 16382098]

[7]. Cummins TR, Dib-Hajj SD, Black JA, Akopian AN, Wood JN, Waxman SG. A novel persistent tetrodotoxin-resistant sodium current in SNS-null and wild-type small primary sensory neurons. J Neurosci 1999;19(24):RC43. [PubMed: 10594087]

[8]. Dib-Hajj S, Black JA, Cummins TR, Waxman SG. NaN/Nav1.9: a sodium channel with unique properties. Trends Neurosci 2002;25(5):253–259. [PubMed: 11972962]

[9]. Dib-Hajj SD, Black JA, Waxman SG. NaV1.9: a sodium channel linked to human pain. Nat Rev Neurosci 2015;16(9):511–519. [PubMed: 26243570]

[10]. Dib-Hajj SD, Tyrrell L, Black JA, Waxman SG. NaN, a novel voltage-gated Na channel, is expressed preferentially in peripheral sensory neurons and down-regulated after axotomy. Proc Natl Acad Sci U S A 1998;95(15):8963–8968. [PubMed: 9671787]

[11]. Dib-Hajj SD, Tyrrell L, Cummins TR, Black JA, Wood PM, Waxman SG. Two tetrodotoxin-resistant sodium channels in human dorsal root ganglion neurons. FEBS Lett 1999;462(1–2):117–120. [PubMed: 10580103]

[12]. Fang X, Djouhri L, McMullan S, Berry C, Waxman SG, Okuse K, Lawson SN. Intense isolectin-B4 binding in rat dorsal root ganglion neurons distinguishes C-fiber nociceptors with broad action potentials and high Nav1.9 expression. J Neurosci 2006;26(27):7281–7292. [PubMed: 16822986]

[13]. Gold MS, Thut PD. Lithium increases potency of lidocaine-induced block of voltage-gated na(+) currents in rat sensory neurons in vitro. J Pharmacol Exp Ther 2001;299(2):705–711. [PubMed: 11602684]

[14]. Han C, Yang Y, Te Morsche RH, Drenth JP, Politei JM, Waxman SG, Dib-Hajj SD. Familial gain-of-function Nav1.9 mutation in a painful channelopathy. J Neurol Neurosurg Psychiatry 2017;88(3):233–240. [PubMed: 27503742]

[15]. Hartung JE, Moy JK, Loeza-Alcocer E, Nagarajan V, Jostock R, Christoph T, Schroeder W, Gold MS. Voltage-gated calcium currents in human dorsal root ganglion neurons. Pain 2022;163(6):e774–e785. [PubMed: 34510139]

[16]. Hockley JR, Boundouki G, Cibert-Goton V, McGuire C, Yip PK, Chan C, Tranter M, Wood JN, Nassar MA, Blackshaw LA, Aziz Q, Michael GJ, Baker MD, Winchester WJ, Knowles CH, Bulmer DC. Multiple roles for NaV1.9 in the activation of visceral afferents by noxious inflammatory, mechanical, and human disease-derived stimuli. Pain 2014;155(10):1962–1975. [PubMed: 24972070]

[17]. Hoffmann T, Kistner K, Carr RW, Nassar MA, Reeh PW, Weidner C. Reduced excitability and impaired nociception in peripheral unmyelinated fibers from Nav1.9-null mice. Pain 2017;158(1):58–67. [PubMed: 27780178]

[18]. Huang J, Estacion M, Zhao P, Dib-Hajj FB, Schulman B, Abicht A, Kurth I, Brockmann K, Waxman SG, Dib-Hajj SD. A Novel Gain-of-Function Nav1.9 Mutation in a Child With Episodic Pain. Frontiers in neuroscience 2019;13:918. [PubMed: 31551682]

[19]. Huang J, Han C, Estacion M, Vasylyev D, Hoeijmakers JG, Gerrits MM, Tyrrell L, Lauria G, Faber CG, Dib-Hajj SD, Merkies IS, Waxman SG. Gain-of-function mutations in sodium channel Na(v)1.9 in painful neuropathy. Brain 2014;137(Pt 6):1627–1642. [PubMed: 24776970]

[20]. Huang J, Vanoye CG, Cutts A, Goldberg YP, Dib-Hajj SD, Cohen CJ, Waxman SG, George AL, Jr. Sodium channel NaV1.9 mutations associated with insensitivity to pain dampen neuronal excitability. J Clin Invest 2017;127(7):2805–2814. [PubMed: 28530638]

[21]. Leipold E, Liebmann L, Korenke GC, Heinrich T, Giesselmann S, Baets J, Ebbinghaus M, Goral RO, Stödberg T, Hennings JC, Bergmann M, Altmüller J, Thiele H, Wetzel A, Nürnberg P, Timmerman V, De Jonghe P, Blum R, Schaible HG, Weis J, Heinemann SH, Hübner CA, Kurth I. A de novo gain-of-function mutation in SCN11A causes loss of pain perception. Nat Genet 2013;45(11):1399–1404. [PubMed: 24036948]

[22]. Lin Z, Santos S, Padilla K, Printzenhoff D, Castle NA. Biophysical and Pharmacological Characterization of Nav1.9 Voltage Dependent Sodium Channels Stably Expressed in HEK-293 Cells. PLoS One 2016;11(8):e0161450. [PubMed: 27556810]

[23]. Lolignier S, Amsalem M, Maingret F, Padilla F, Gabriac M, Chapuy E, Eschalier A, Delmas P, Busserolles J. Nav1.9 channel contributes to mechanical and heat pain hypersensitivity induced by subacute and chronic inflammation. PLoS One 2011;6(8):e23083. [PubMed: 21857998]

[24]. Lolignier S, Bonnet C, Gaudioso C, Noël J, Ruel J, Amsalem M, Ferrier J, Rodat-Despoix L, Bouvier V, Aissouni Y, Prival L, Chapuy E, Padilla F, Eschalier A, Delmas P, Busserolles J. The Nav1.9 channel is a key determinant of cold pain sensation and cold allodynia. Cell reports 2015;11(7):1067–1078. [PubMed: 25959819]

[25]. Lu SG, Zhang X, Gold MS. Intracellular calcium regulation among subpopulations of rat dorsal root ganglion neurons. J Physiol 2006;577(Pt 1):169–190. [PubMed: 16945973]

[26]. Luiz AP, Kopach O, Santana-Varela S, Wood JN. The role of Nav1.9 channel in the development of neuropathic orofacial pain associated with trigeminal neuralgia. Mol Pain 2015;11:72. [PubMed: 26607325]

[27]. Maingret F, Coste B, Padilla F, Clerc N, Crest M, Korogod SM, Delmas P. Inflammatory mediators increase Nav1.9 current and excitability in nociceptors through a coincident detection mechanism. J Gen Physiol 2008;131(3):211–225. [PubMed: 18270172]

[28]. Martinez V, Melgar S. Lack of colonic-inflammation-induced acute visceral hypersensitivity to colorectal distension in Na(v)1.9 knockout mice. Eur J Pain 2008;12(7):934–944. [PubMed: 18280187]

[29]. McGaraughty S, Chu KL, Scanio MJ, Kort ME, Faltynek CR, Jarvis MF. A selective Nav1.8 sodium channel blocker, A-803467 [5-(4-chlorophenyl-N-(3,5-dimethoxyphenyl)furan-2-carboxamide], attenuates spinal neuronal activity in neuropathic rats. J Pharmacol Exp Ther 2008;324(3):1204–1211. [PubMed: 18089840]

[30]. Moy JK, Hartung JE, Duque MG, Friedman R, Nagarajan V, Loeza-Alcocer E, Koerber HR, Christoph T, Schröder W, Gold MS. Distribution of functional opioid receptors in human dorsal root ganglion neurons. Pain 2020;161(7):1636–1649. [PubMed: 32102022]

[31]. Moy JK, Loeza-Alcocer E, Gold MS. Electrophysiological Recording Techniques from Human Dorsal Root Ganglion. In: Seal RP, editor. Contemporary Approaches to the Study of Pain: From Molecules to Neural Networks, Vol. 178. New York: Springer, 2022. pp. 115–133.

[32]. Ogata K, Jeong SY, Murakami H, Hashida H, Suzuki T, Masuda N, Hirai M, Isahara K, Uchiyama Y, Goto J, Kanazawa I. Cloning and expression study of the mouse tetrodotoxin-resistant voltage-gated sodium channel alpha subunit NaT/Scn11a. Biochem Biophys Res Commun 2000;267(1):271–277. [PubMed: 10623609]

[33]. Padilla F, Couble ML, Coste B, Maingret F, Clerc N, Crest M, Ritter AM, Magloire H, Delmas P. Expression and localization of the Nav1.9 sodium channel in enteric neurons and in trigeminal sensory endings: implication for intestinal reflex function and orofacial pain. Mol Cell Neurosci 2007;35(1):138–152. [PubMed: 17363266]

[34]. Porreca F, Lai J, Bian D, Wegert S, Ossipov MH, Eglen RM, Kassotakis L, Novakovic S, Rabert DK, Sangameswaran L, Hunter JC. A comparison of the potential role of the tetrodotoxin-insensitive sodium channels, PN3/SNS and NaN/SNS2, in rat models of chronic pain. Proc Natl Acad Sci U S A 1999;96(14):7640–7644. [PubMed: 10393873]

[35]. Priest BT, Murphy BA, Lindia JA, Diaz C, Abbadie C, Ritter AM, Liberator P, Iyer LM, Kash SF, Kohler MG, Kaczorowski GJ, MacIntyre DE, Martin WJ. Contribution of the tetrodotoxin-resistant voltage-gated sodium channel NaV1.9 to sensory transmission and nociceptive behavior. Proc Natl Acad Sci U S A 2005;102(26):9382–9387. [PubMed: 15964986]

[36]. Ritter AM, Martin WJ, Thorneloe KS. The voltage-gated sodium channel Nav1.9 is required for inflammation-based urinary bladder dysfunction. Neurosci Lett 2009;452(1):28–32. [PubMed: 19146922]

[37]. Rugiero F, Mistry M, Sage D, Black JA, Waxman SG, Crest M, Clerc N, Delmas P, Gola M. Selective expression of a persistent tetrodotoxin-resistant Na+ current and NaV1.9 subunit in myenteric sensory neurons. J Neurosci 2003;23(7):2715–2725. [PubMed: 12684457]

[38]. Rush AM, Waxman SG. PGE2 increases the tetrodotoxin-resistant Nav1.9 sodium current in mouse DRG neurons via G-proteins. Brain Res 2004;1023(2):264–271. [PubMed: 15374752]

[39]. Tate S, Benn S, Hick C, Trezise D, John V, Mannion RJ, Costigan M, Plumpton C, Grose D, Gladwell Z, Kendall G, Dale K, Bountra C, Woolf CJ. Two sodium channels contribute to TTX-R sodium current in primary sensory neurons. Nature Neurosci 1998;1(8):653–655. [PubMed: 10196578]

[40]. Touska F, Turnquist B, Vlachova V, Reeh PW, Leffler A, Zimmermann K. Heat-resistant action potentials require TTX-resistant sodium channels NaV1.8 and NaV1.9. J Gen Physiol 2018;150(8):1125–1144. [PubMed: 29970412]

[41]. Zhang X, Hartung JE, Friedman RL, Koerber HR, Belfer I, Gold MS. Nicotine Evoked Currents in Human Primary Sensory Neurons. J Pain 2019.

[42]. Zhang X, Priest BT, Belfer I, Gold MS. Voltage-gated Na+ currents in human dorsal root ganglion neurons. eLife 2017;6.

[43]. Zhang XL, Lee KY, Priest BT, Belfer I, Gold MS. Inflammatory mediator-induced modulation of GABAA currents in human sensory neurons. Neuroscience 2015;310:401–409. [PubMed: 26415765]

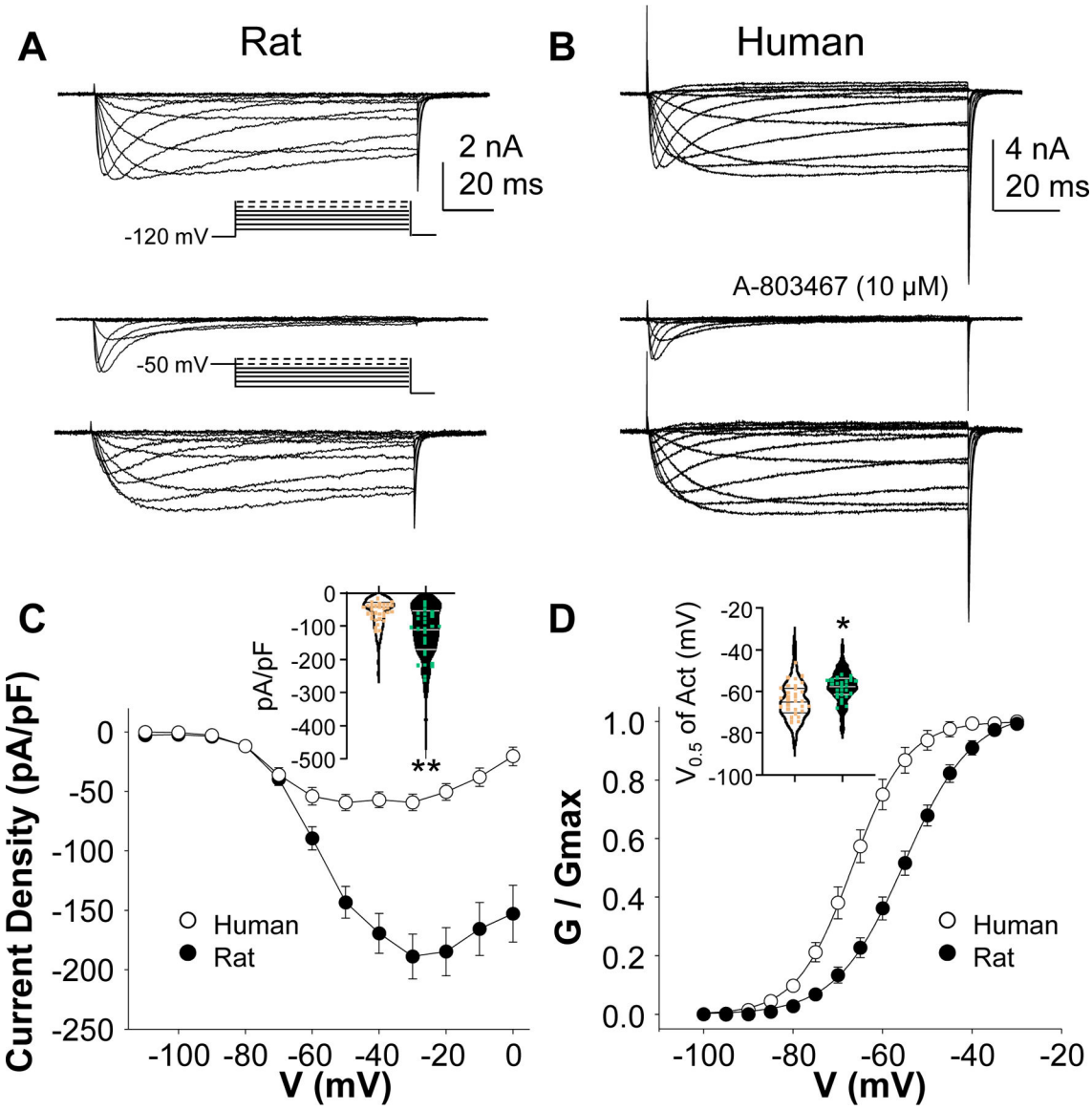

Figure 1.

Persistent low threshold sodium currents (I_{Na}) present in rat and human sensory neurons. **A**. Total tetrodotoxin (TTX) resistant voltage-gated I_{Na} was evoked in rat sensory neurons from a holding potential of −120 mV in the presence of 300 nM TTX (top trace). NaV1.8 currents were isolated from total currents by changing the holding potential to ~−50 mV (middle traces). NaV1.9 currents were isolated by subtracting NaV1.8 currents from total current (bottom traces). **B**. A second method used to isolate NaV1.9 currents is illustrated in a human DRG neuron, where total TTX-resistant current (top traces) was evoked before the application of A-803467 (10 μM) (bottom traces). In this case, NaV1.8 could be digitally isolated (middle traces) by subtracting the current evoked in the presence of A-803467 from total current. **C**. Pooled I-V data collected as illustrated in A, and B, were normalized to membrane capacitance. Current density was significantly higher in rat than human sensory neurons. *Inset*: Current density at −50 mV from all neurons studied was also greater in rat

than human. Violin plots are of all human (open) and rat (closed) neurons studied (with median and 25^{th} and 75^{th} quartile indicated), while the overlaying dot plots are of the mean from each donor (tan) or rat (green). The current density was larger in rat than human neurons, even at −50 mV, despite the more depolarized G-V curve. **D**. Tail currents, or instantaneous G-V data were used to generate G-V curves for each neuron. Each curve was than fitted with a modified Boltzmann equation to estimate G_{max}, the potential for half activation ($V_{0.5}$), and the slope of the G-V curve. G-V data for each neuron was then normalized to the fitted G_{max} prior to pooling. *Inset*, fitted $V_{0.5}$ data for all neurons in which I-V/G-V data were collected, are plotted in a manner comparable to the current density data in C. There was a small but significant different between species with respect to the $V_{0.5}$ of activation. In this and subsequent figures ** is $p < 0.01$ and * is $p < 0.05$, where the n used for comparisons was the number of rats or donors.

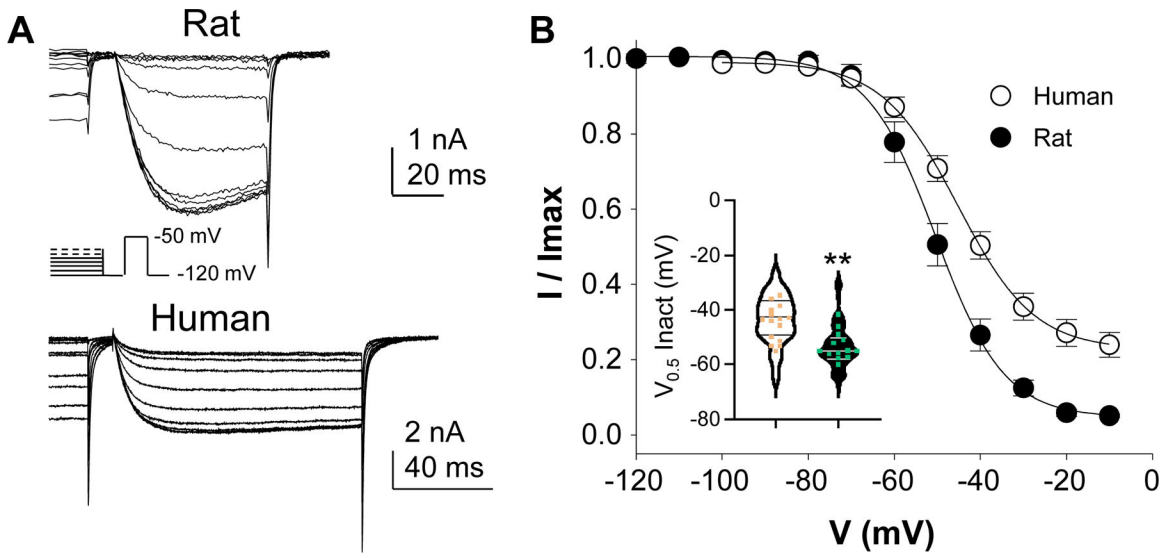

Figure 2.

Relatively fast inactivation of NaV1.9 currents evoked in rat and human sensory neurons. **A**. A 500 ms conditioning pulse to potentials between −120 mV and −10 mV in 10 mV steps was used to assess the voltage-dependence of inactivation in rat (top traces) and human (bottom traces) sensory neurons. A brief (10 ms) hyperpolarizing voltage step to −120 mV was used to close channel prior to assessing the current evoked with a voltage step to −50 mV. Inactivation data from each neuron were fitted with a modified Boltzmann curve to estimate the maximal current (I_{max}), the voltage of half inactivation ($V_{0.5}$), the slope of the inactivation curve, and the fraction of non-activatable current. The difference in the fraction of non-inactivatable current between rat and human neurons was significant ($p < 0.01$), as was the V0.5 of inactivation, which was more hyperpolarized in rat neurons (Inset).

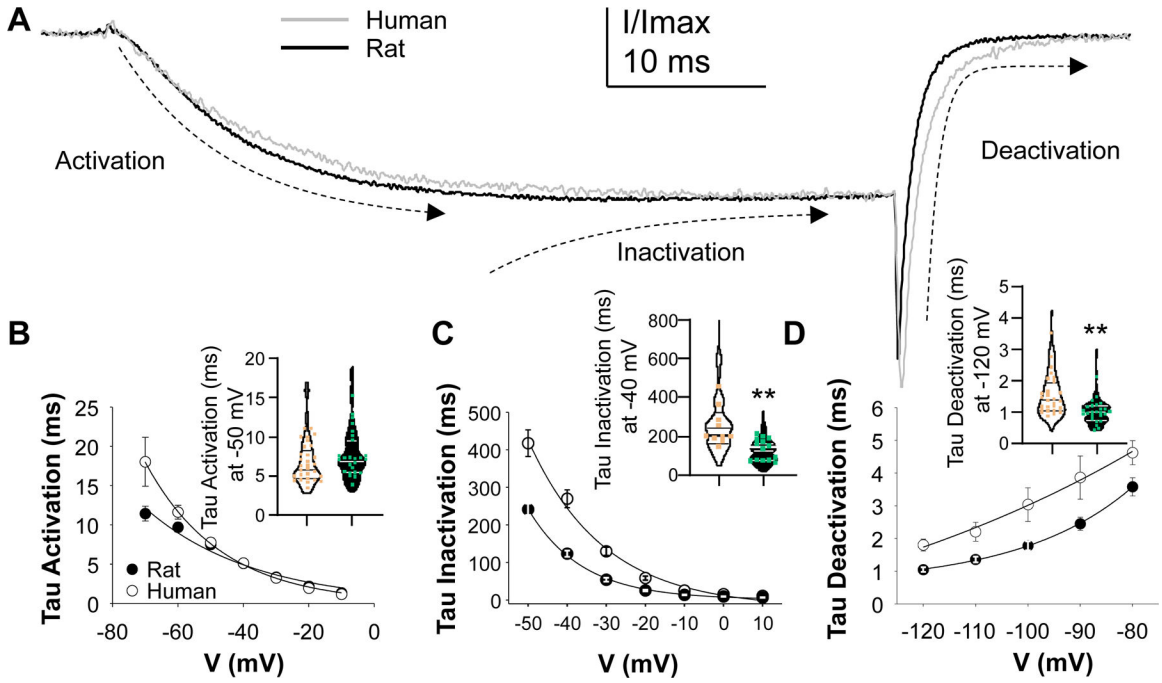

Figure 3.

Kinetics of NaV1.9 current activation, inactivation, and deactivation. **A**. NaV1.9 current evoked from a rat (black trace) and a human (grey trace) sensory neuron have been scaled to peak current. As suggested by the current traces, rates of current activation are comparable, but rates of deactivation are faster in rat sensory neurons. **B**. The time constant, or tau, of current activation, is plotted as a function of test potential. *Inset*: Pooled inactivation data for current evoked at −40 mV is plotted as in Figure 1C. **C**. Current inactivation is significantly faster in rat sensory neurons. **D**. The time constant, or tau of current deactivation is faster in rat than human sensory neurons. Inset: Pooled deactivation data for current evoked at −50mV with a return to −120 mV, plotted as in the inset to Figure 1C. Current deactivation is significantly faster in rat sensory neurons.

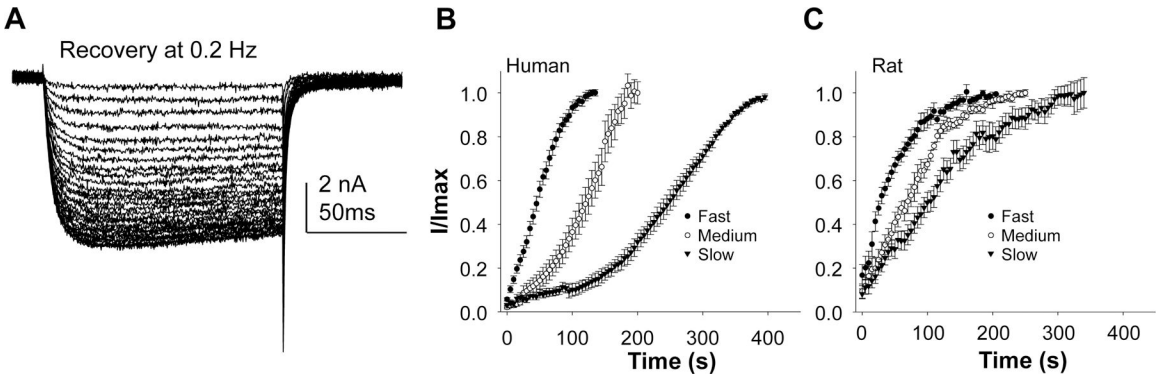

Figure 4.

Recovery from slow inactivation. **A**. Recovery from slow inactivation was monitored with a test pulse to −50 mV evoked at 0.2Hz after the return of the holding potential to −120 mV following 3 minutes at −50 mV to drive slow inactivation of NaV1.9. **B**. Recovery was best described in human sensory neurons by a sigmoidal process, where recovery in the majority of neurons studied was considered fast (i.e., 90% of max within 100 s), although there were subpopulations in which recovery was medium (i.e., 90% of max within 200 s) or slow (i.e., 90% of max in >300 s. **C**. Recovery of currents in rat sensory neurons was best described with a single exponential, where again, there were neurons that recovered with a time course that would be considered fast, medium, and slow by the criteria used in human sensory neurons. However, the majority of neurons from rat recovered slowly from slow inactivation.

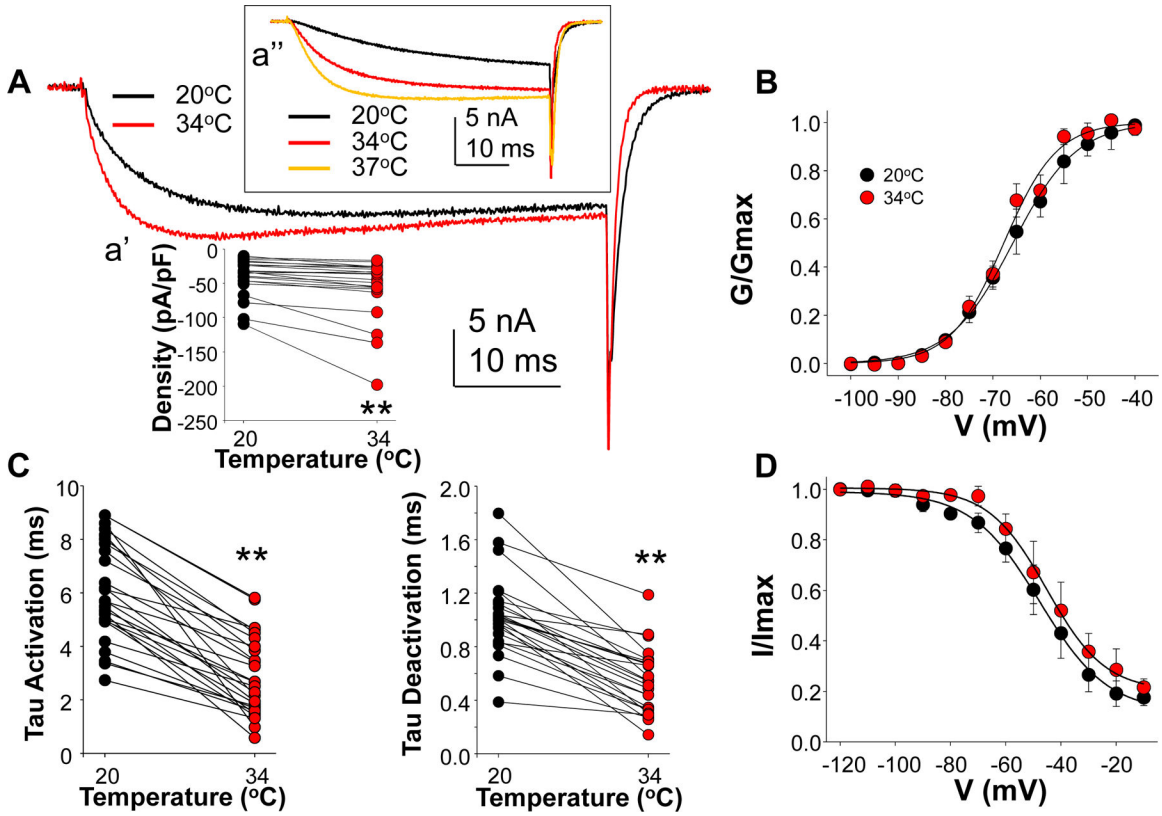

Figure 5:

Impact of temperature on NaV1.9 currents. **A**. NaV1.9 currents in a human sensory neuron evoked at −50 mV at 20°C (black trace) and 34°C (red trace). *Inset a'*: current density at −50 mV in individual human neurons evoked at 20°C and 34°C. The increase in current density is significant. Inset a": current evoked in a rat DRG neuron at −50 mV with a bath temperature at 20°C (black trace), 34°C (red trace), and 37°C (orange trace). **B**. There was no influence of temperature on G-V curves for current evoked in human DRG neurons at 20°C and 34°C, which were normalized to G_{max} as described in Figure 1. **C.** Time constant (tau) of current activation and deactivation at 20°C and 34°C. Rates of both channel opening and closing were significantly increased with an increase in temperature. **D**. There was no influence of temperature on the voltage-dependence of current inactivation in human sensory, which was normalized to the fitted I_{max} as described in Figure 2.

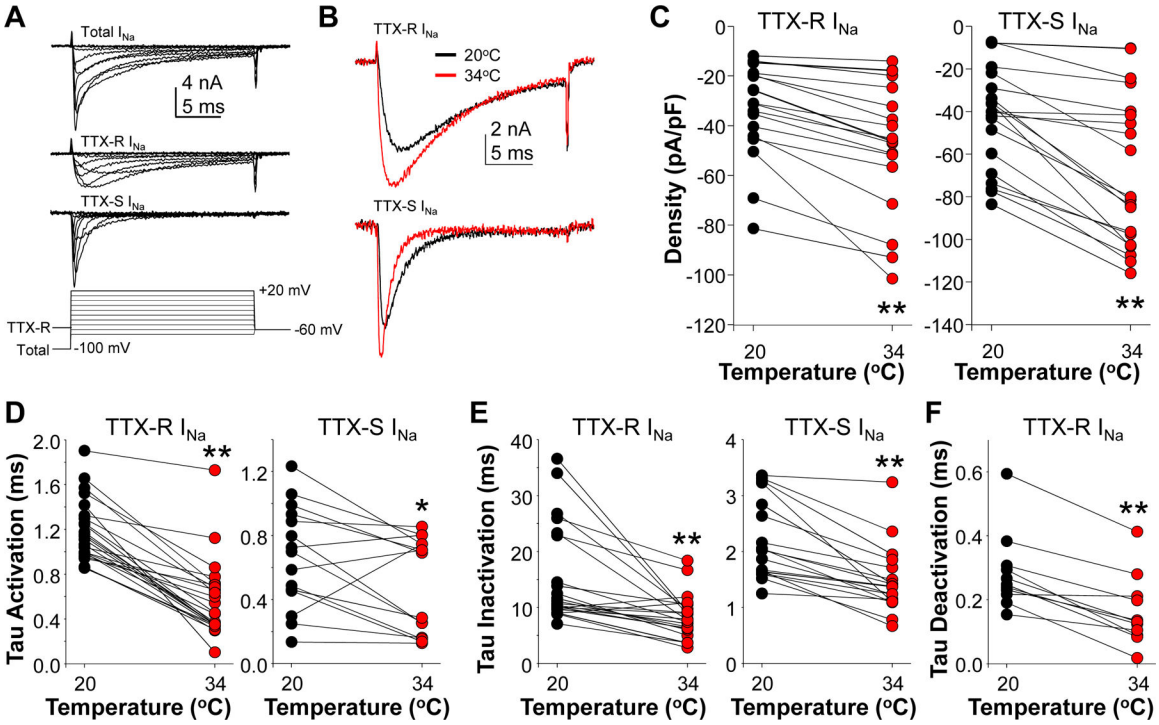

Figure 6:

Impact of temperature on TTX-S and NaV1.8 (TTX-R I_{Na}) currents in human DRG neurons. TTX-S and TTX-R I_{Na} were isolated in human and rat (not shown) sensory neurons with a voltage-protocol involving a 500 ms hyperpolarizing step to −100 mV to recover TTX-S currents from inactivation. **A**. Current evoked following the pre-pulse to −100 mV was considered Total current (Total I_{Na}, top traces). If the pre-pulse was changed to −50 mV, TTX-R I_{Na} was the only currents evoked (middle traces). TTX-S currents were isolated by digitally subtracting NaV1.8 current from Total I_{Na} (bottom traces). **B**. Peak NaV1.8 current (top traces) and TTX-S current (bottom traces) in a human sensory neuron evoked at 20°C (black trace) and 34°C (red trace). **C**. Increasing the bath temperature from 20°C to 34°C resulted in a significant increase in the peak density of both TTX-R (left panel) and TTX-S (right panel) I_{Na} in human sensory neurons. Increasing bath temperature from 20°C to 34°C also increased activation rats (**D**) and inactivation rates (**E**) for both TTX-R and TTX-S I_{Na}, as well as the deactivation rates for TTX-R I_{Na} (**F**). Comparable results were obtained for rat neurons (not shown).

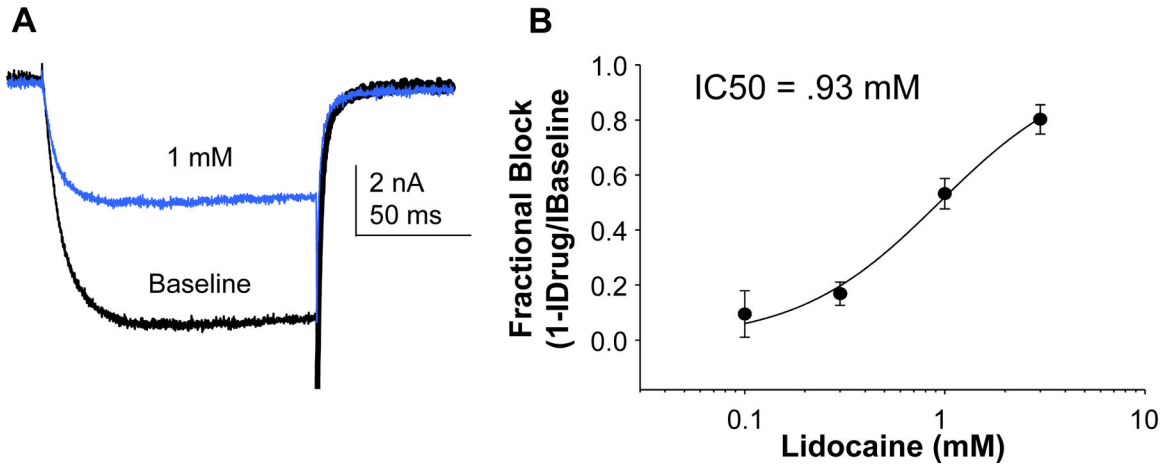

Figure 7.

Persistent current in human sensory neurons is relatively insensitive to lidocaine. **A**. Current evoked in a human sensory neuron before (Baseline – black trace) and after (1 mM) the application of 1 mM lidocaine (blue trace). **B**. Concentration response data for human sensory neurons exposed to lidocaine. Data are evoked current at −50 mV after a stable value had been reached. Pooled data were fitted with a modified Hill equation to estimate the IC_{50} of lidocaine.

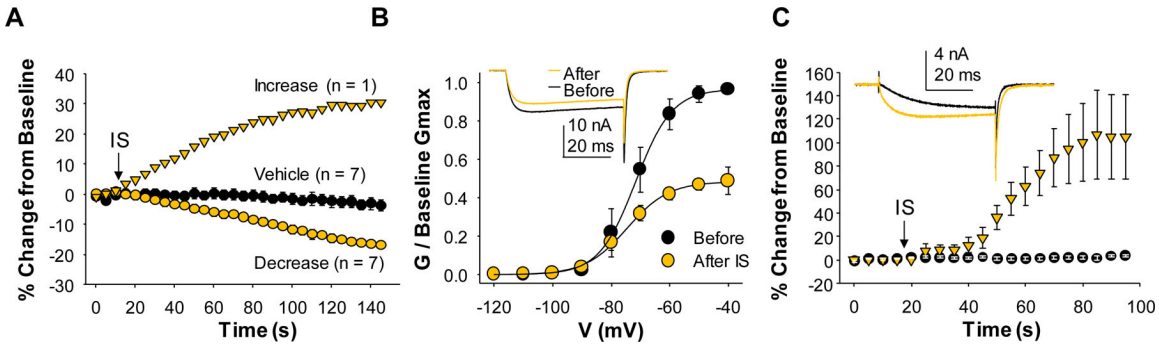

Figure 8.

The impact of inflammatory soup (IS) on NaV1.9 currents in human and rat sensory neurons. **A**. Persistent current was evoked at −50 mV in human sensory neurons before and then after an IS consisting of PGE_2 (1 μM), histamine (1 μM), serotonin (1 μM), and bradykinin (10 μM) or vehicle. Current decreased in 7 of 8 neurons tested with IS, whereas no change was detected in vehicle treated neurons. An increase in current was observed in one of the 8 neurons tested. **B**. The decrease in current was associated with an apparent decrease in G_{max}, with no changes in either the voltage-dependence of activation of the slope of the G-V curve. **C**. In rat sensory neurons, IS, but not vehicle, was associated with a consistent increase in current evoked at −50 mV.